First Reviewer

We appreciate the referee's comments as they were both helpful and enlightening. All the highlighted typos have been corrected but not addressed in this document in order not to overextend the response. Only major changes and clarification notes are presented. The numeration has changed and the figures' and tables' numeration refers to the last version of the manuscript.

Page 1: Abstract.

Do you mean the distance from the centre of a square cell? The same in the following when you speak about distance from a cell.

The abstract has been modified in order to use a more concise language: every reference to the cell distance has now been regarded as distance to the centre of the grid cell to avoid any ambiguity (p.1 line 5, p.3 line 58, etc.).

The word "oscillation" refers to alternate episodes of increase and decrease of the probability, but it does not seem appropriate to the results shown in this paper.

Regarding the use of the word oscillation, we agree that it is no appropriate in this context so the whole sentence has been changed:

Lines 14-17:

"*In the case of Italy, the annual probability of exceedance increases significantly, but in the case of Spain not all the earthquakes have an associated increase in the exceedance probability.*"

Page 5: 2.1 Smoothing kernel

Please, give some references.

This function does not seem a 2D Gaussian function. The maximum is not in a point, but on a circle of radius "mu".

Lines 115-116:

The description of the smoothing kernel has been changed to correctly describe its effects and a citation to a similar function has been added:

"*For this work, a well-known smoothing function **(Frankel, 1995)** has been selected to smooth the gridded seismicity, the 1D Gaussian function **(Eq. 6)**:*"

When the distance from the point in which the seismic activity rate is being computed to the centre of the spatial grid cell that contributes to that computation is calculated, the variable of interest becomes 1D rather than 2D (if the longitude and latitude of each point where considered) and the expression of the smoothing function becomes simpler.

Lines 119-121:

The description of the smoothing kernel has been changed to the following:

$$f(r) = A \cdot \exp\left(-\frac{(r-\mu)^2}{2 \cdot \sigma^2}\right)$$

*"where **r** is the distance between the centre of the spatial grid cells and the centre of the cell in which the seismic activity is being computed, **A** is the normalization constant, **μ** is the parameter that controls the **r** value at which the maximum of the function is reached, and **σ** controls the dispersion of the function around the maximum value."*

This has been done to avoid a direct relationship between the parameters on the smoothing function to those of the normal distribution PDF before arriving to the discussion section.

Additionally, a new subsection has been created to illustrate the difference between the $\boldsymbol{\mu = 0}$ and $\boldsymbol{\mu = d_{f_i}}$ cases, as well as an example of code implementation.

There is confusion between the mean and the modal value (maximum of the distribution).

- **First moment of the distribution, μ** has been renamed to **Geophysical meaning of the parameter μ** and the contents of the subsection have been rewritten in order for them to be more clearly defined.

"The meaning of this parameter within the context of the seismic activity smoothing for this model is the distance from a given cell centre to the point(s) in which the probability of having an earthquake is higher.

*It is common to find that the value of this parameter is set to zero **(Frankel, 1995; Helmstetter et al., 2006; Hiemer et al., 2014)**, as the maximum probability of having an earthquake is where it has already happened before. So, the smoothing function has its maximum value in the cell in which the seismic activity rate is being smoothed. This constitutes the first option regarding this parameter: **μ = 0**.*

An alternative model is proposed, where the maximum probability is set at the location of the nearest seismic sources. For this to be implemented, the minimum distance between the point in which seismic activity rate is being computed and the location of the nearest seismic source is calculated and named in this work from now on as $\boldsymbol{d_{f_i}}$. So, the second option for the parameter value is $\boldsymbol{\mu = d_{f_i}}$.

For areas in which the tectonic structures are only present in part of the region, a hybrid approach may be applied by using cut-off distance. This cut-off distance may be calculated as follows:

$$d_c = \bar{d} + 2 \cdot \sigma_d$$

where $\boldsymbol{d_c}$ is the cut-off distance, $\boldsymbol{\bar{d}}$ stands for the mean value of the distance between all the structures, and $\boldsymbol{\sigma_d}$ is the standard deviation for all these distances.

If the distance from the centre of the spatial grid cell to the nearest fault is higher than the cut-off distance then ***μ = 0****. Otherwise, it will be set to* d_{f_i}*"*

It does not seem to me that it is the dominant factor of the dispersion. There is also a physical dispersion.

- **Second moment of the distribution, σ** has been renamed to **Geophysical meaning of the parameter σ** and the contents of the subsection have been rewritten in order for them to be more clearly defined.

"This parameter accounts for the dispersion of the values of the distribution around the mean value. That is to say, how far one might expect to find earthquakes around the most probable value (of distance). Therefore, we have considered that this second parameter is related to the accuracy of earthquake's epicentre measurement. This means that it would depend on the methodologies and instrumentation used for the calculation of the epicentre, and thus, on both the year and the location of the catalogue.

It should be noted that ***σ*** *may depend on other geophysical parameters such as the characteristics of ground, the style of faulting and/or the tectonic stress regime, to cite a few. Nevertheless, in this work only the influence of the uncertainty in the epicentre's location will be considered in the smoothing process.*

As in the previous section, two different options regarding the epicentre uncertainty, ***ε****, have been considered: either it depends on the year of occurrence (*ε_1*), or it is constant and computed as the mean value of the epicentral uncertainty for all the events (*ε_2*). "*

A new subsection has been added to show examples of the smoothing kernel implementation and a figure showcasing how the smoothing works is presented:

2.1.3 Examples of the smoothing kernel implementation

"In this section, some examples of how the smoothing kernels works are shown. There are three main different manners in which this smoothing is applied:

- *Usual 1D Gaussian filter,* $\mu = 0$

This is the case when using models 2 and 3 also when the distance from the centre of the spatial grid cell in which the seismic activity rate is computed to the nearest fault is greater than d_c *as defined in the section* ***2.1.1.*** *An example can be seen in* ***Figure 1a.***

- *Single fault,* $\mu \neq 0$

When the nearest fault is closer than d_c *from the centre of the spatial grid cell then the resulting function will provide a ring-shaped smoothed activity, the width of which will depend on* ***σ****. Only the section of this ring in which the fault is located will be used in the smoothing. This can be achieved by considering the* ***n*** *closest points*

*to the spatial grid cell centre and then computing the angles to define the ring arc (**Figure 1b**).*

- *Several faults, $\mu \neq 0$*

*This case is a generalization of the former with the exception that when spatial grid cell's centre is in between faults and at similar distances, then the full ring will be used as smoothing function (**Figure 1d**). On the other hand, if the distance to both faults is similar, but the spatial grid cell's centre is not in between the faults then the resulting smoothing is a ring arc (**Figure 1c**).”*

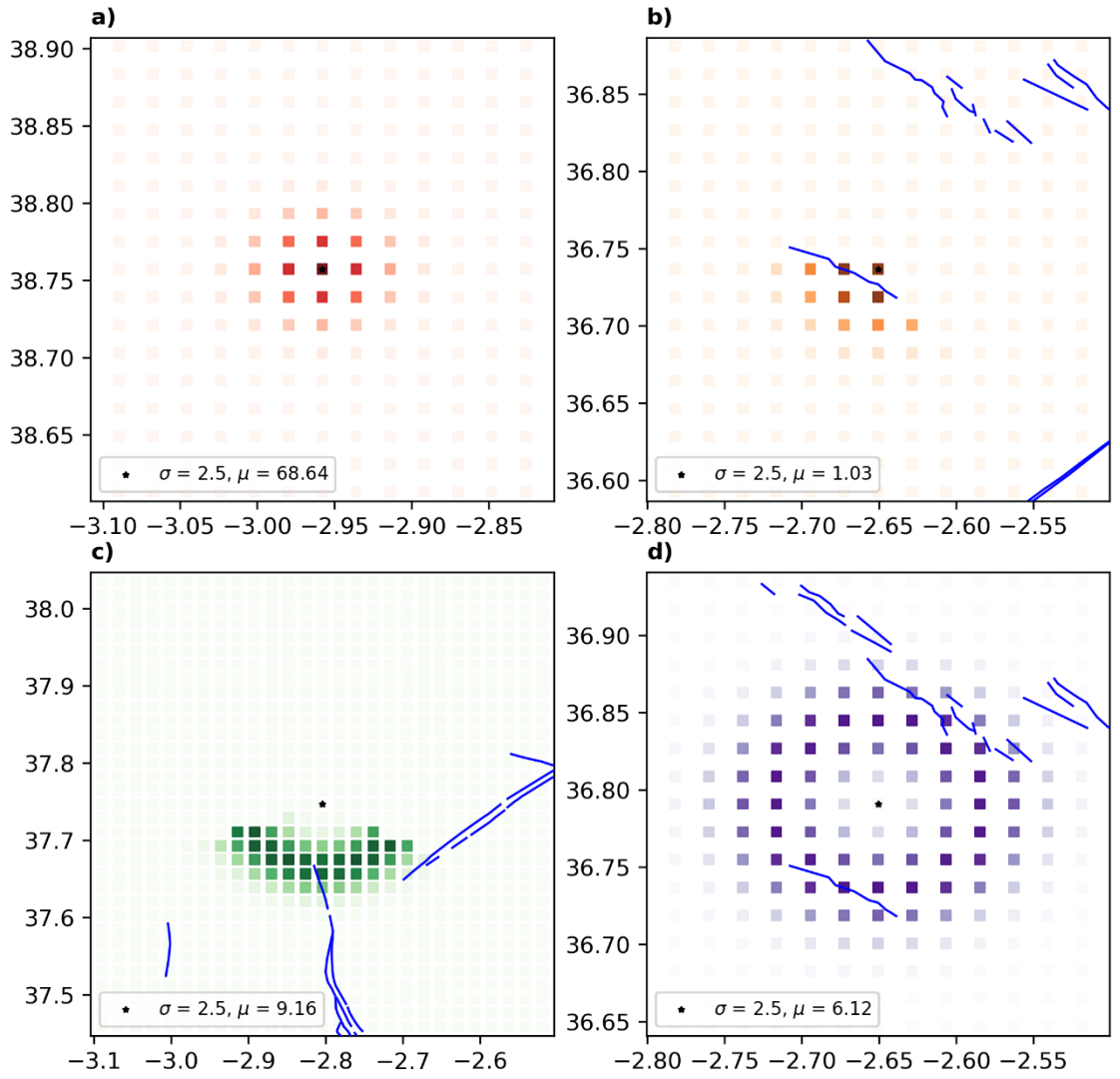

Figure 1. a) Smoothing function for $\mu = 0$. b) Smoothing function for $\mu \neq 0$ and a single fault. c) Smoothing function for $\mu \neq 0$ and several faults at similar distances. d) Smoothing function for $\mu \neq 0$ and the spatial grid cell in between faults at similar distances. The blue lines show the fault traces. In this example d_c equals 48 km.

Statistical methods were introduced for declustering without removing events from a catalogue, but assigning to each earthquake a weight equal to the probability of being independent These methods make use of the Epidemic (ETAS) model. See, e.g.:

ZHUANG, J., OGATA, Y., and VERE-JONES, D. (2002), Stochastic declustering of space-time earthquake occurrences, J. Am. Stat. Ass. 97, 458, 369–380.

MARSAN, D. and LONGLINE´, O. (2008), Extending earthquakes' reach through cascading, Science 319, 1076–1079.

Console, R., Jackson, D.D., Kagan, Y.Y. (2010). Using the ETAS model for catalog declustering and seismic background assessment. Pure Appl. Geoph., 10.1007/s00024-010-0065-5.

These algorithms, based on parameters whose value is established by the maximum likelihood, avoid the difference between declustered catalogues obtained from a subjective choice of different algorithms.

Page 8: **2.2 Cluster identification and seismicity smoothing**

A paragraph has been introduced discussing the methodology and taking into account the references.

"First, the spatial grid is defined by creating a rectangle spanning the maximum and minimum longitudes and latitudes of the catalogue with the desired resolution. Then, all the events of the catalogue must be assigned to each cell. This is done by calculating the minimum distance of each event to all the spatial grid cell's centres.

One of the most important steps regarding the activity rate calculation in this work, is the identification of the seismic clusters present in the area for the selected period of time. As indicated in the introduction, we do not pretend to remove the foreshocks and aftershocks but to identify the main event and all related events in the corresponding cluster.

To do so, even though Epidemic Type Aftershock Sequence (ETAS) model allows to assign to each event the probability of being an aftershock ***(Zhuang et al., 2002; Marsan and Longline, 2008; Console et al., 2010)*** *in this work we have decided to select a non-stochastic method based on the performance classifying events of a relevant seismic series."*

Additionally, the procedure in which the methods are tested has been expanded by computing the confusion matrix for all the methods given the knowledge on the Lorca's series. Now after **Table 6** in **page 19** is presented:

"Considering that ***Cabañas et al. (2011)*** *carried out a detailed study on the 2011 Lorca's earthquake seismic series, we have used their results to validate the best algorithm. According to them, the cluster corresponding to Lorca's series, from 11 May 2011 until 19 July 2011, is composed of 146 events (including the foreshock, the main shock and the aftershocks). In order to test the performance of the declustering methods, the confusion matrices for each one have been computed. In the area of study, a total of 249 events have been recorded, which means a total of 103 background events should be identified. For this analysis, all the events classified in a cluster different from Lorca series' have been considered as*

*background events for simplicity. **Figure 9** shows that GK74 method is the most adequate (with a 94.43% mean for the metrics compared with the 92.88% for RJ and a 74.54% for A) and also the one that is able to identify more events belonging to Lorca series."*

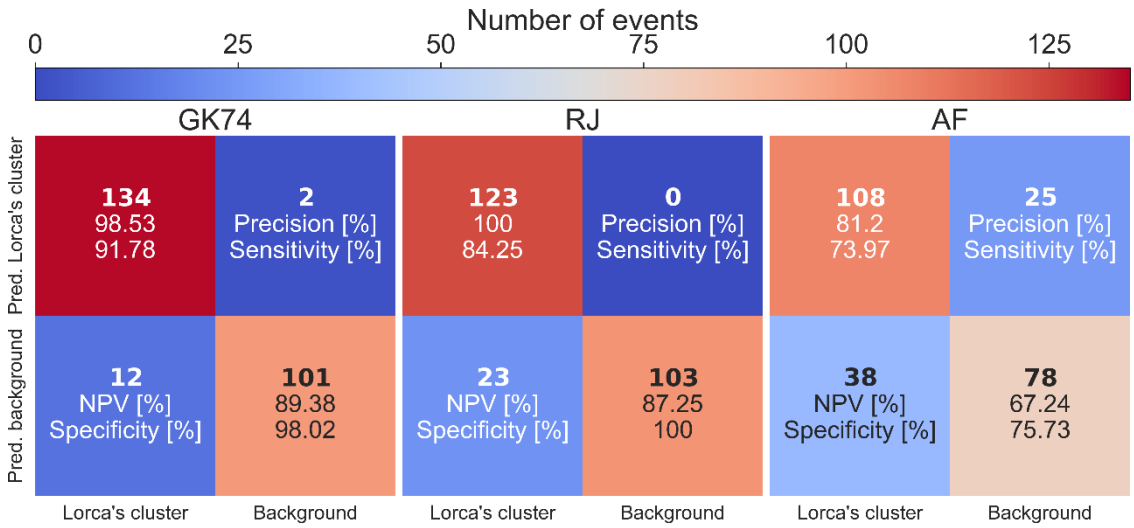

Figure 9. Confusion matrices for the tested declustering methods. Inside each square, the number of events (bold) and some metrics computed using the data are presented (NPV stands for Negative Predictive Value).

The maps of this figure should be redrawn with a larger size.

Page 11: Figure 3

The maps in the **Figure 3** have been resized so the features can be clearly seen. And the size in the draft has also been increased from 8.3 cm to 12 cm. It has been checked that the legend items can be read at 100% zoom value in the pdf version of the draft and other text processing software.

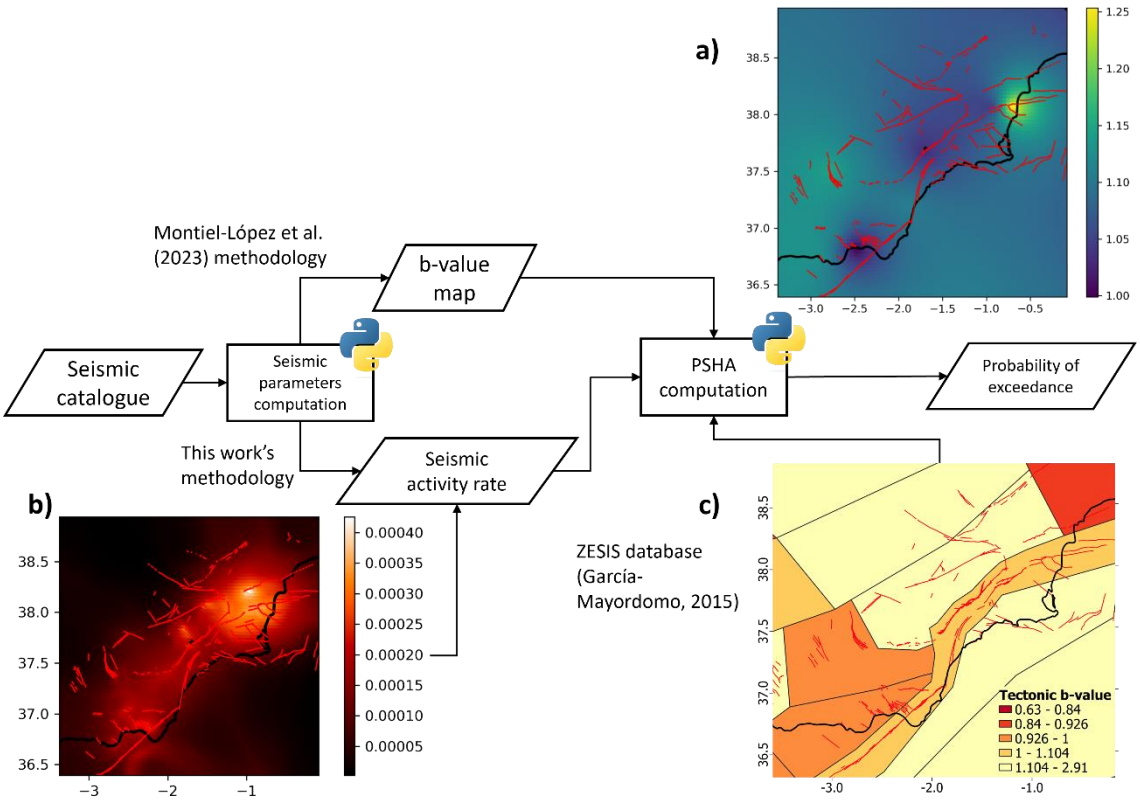

Too long sentence.

Page 10: **2.4. Exceedance probability calculation**

Lines 219-224:

We agree that the sentence is too long, and it has been rewritten:

Our goal is to investigate if the changes in the seismic activity and b-value time series can be observed as a trend in the PSHA results. In the case such trends are observed, this methodology could be used for OEF. For this reason, the temporal evolution of the annual probability of exceedance (PoE) of a background PGA corresponding to a 475 years return period (i.e., 0.002 PoE) has been computed as a time-dependent value. The results have been expressed as a relative change (RC in percentage change, ***Eq. 9****) between background annual exceedance probability (long-term value) and the time-dependent annual exceedance probability.*

Do you mean that the background value is updated in time by the seismic normative?

Line 224-227:

The sentence has been rewritten to avoid any ambiguity and placed just before ***Eq. 9*** as it is related to the background value used to calculate the RC:

Depending on the country, the background (long-term) PGA value may have been updated in the corresponding seismic hazard studies. This could be due to the

occurrence of new damaging earthquakes or improvements in the seismic knowledge of a region, amongst other reasons. In case such changes have been made, a new background PGA value has been computed using the data up until the year the seismic hazard information was updated.

It is well known that foreshock activity occurred in the weeks prior to the Aquila earthquake, with a notable increase just few days before. It is important to clarify if the increase in the exceedance probability is caused by this foreshock activity.

Page 14: **3.1.2 Results**

Lines 260-266:

In the case of the L'Aquila earthquake the foreshock activity allows to see clear changes in PoE as the earthquake preceding the mainshock has magnitude greater than Mw 4.0. That is one of the reasons why we decided to weight down the not independent events rather than eliminating them from the catalogue. The sentence has been rewritten in order to relate the changes in the RC prior the L'Aquila earthquake to the foreshock activity:

*"**Figure 5** (Model 1t) presents a moderate increase in the annual exceedance probability (25%) one month before L'Aquila earthquake occurred, and not only the annual but also the monthly variation of relative change reaches values higher than 35%. This sudden change is most probably due to the foreshock activity that preceded the mainshock, as a 4.1 M_L ground motion occurred on 30 March 2009."*

Table 5 reports only five earthquakes of the seven. Why?

Page 16: **3.2.1 Catalogue preparation and parameters for computation**

Lines 276-279:

The sentence has been rewritten in order to explain the choice of the 5 earthquakes:

*"Additionally, in the last 25 years, South-eastern Spain has suffered seven earthquakes with Mw greater than or equal to 4.5 (**Table 5** and **Figure 8** present only those classified as mainshocks and located in the area of study), being the 2011 Lorca earthquake the most relevant since it was the most recent earthquake causing damage to buildings and injuries to the population."*

Page 13: **Figure 4**

Caption line 2:

The word *tectonic* has been omitted as it is not correct. It was a reference to the tectonics' zone b-value, which is redundant and can induce misunderstanding. All the sentences in which the adjective *tectonic* precedes b-value have been omitted.

Better with respect to which criterion?

Page 21: 3.2.2 Results

Lines 332-336:

The sentence has been rewritten as it was neither accurate nor explanatory. The final sentence refers to the figures for the models 2t and 3t (as the one presented in ***Figure 12*** is the comparison between all the models).

*"After computing the time-dependent PSHA for the different models shown in **Table 9**, we have observed that although all the graphs show similar behaviour for the RC, Model 1t provides greater annual and monthly variations of the RC for some of the earthquakes than the rest, similarly to Italy's case study. Therefore, with the exception of the fixed models (models 1f, 2f and 3f) where we present a general comparison them, we will present the results of Model 1t in this section along with figures comparing all three models. The stand-alone figures for the models 2t and 3t can be found in the* **Appendix** *section."*

Please, explain better how you justify this statement.

Page 22: 3.2.2 Results

Lines 357-362:

The paragraph has been modified with a further explanation. The results presented in **Figure 10**, the comment of which is presented in this paragraph, will also be related to the ones from the time-dependent models (1t, 2t and 3t) in the conclusions.

"It seems that the use of a constant b-value coupled with a time-dependent seismic activity rate leads to a RC that decrease over time with a constant rate and sudden increases mainly due to changes in the background PGA values. This behaviour is due to the update of this parameter depending on the period of the catalogue, which is increased a month at a time (as it was the selected minimum time step for this area). We find that this approach is not appropriate towards earthquake forecasting for areas with low to moderate seismicity. This uniform behaviour potentially rules out the possibility of finding any metrics for OEF.

It is important to distinguish if the sharp increase includes the data of the Mula earthquake or it includes only data before the earthquake. It makes a big difference, which must be clarified.

Lines 364-377:

Mula earthquake occurs after the RC increase mentioned in the manuscript. Nevertheless, this has been corrected as this change is not the one to be addressed when discussing the results. The change that now appears in the discussion ranges from -75% to -60% that is seen from June 1998 on. The sudden change seen from December 1998 to January 1999 is an artifact due to the base change. This has been now explained and it is the reason why two other metrics have been selected

(monthly and annual variations). This is not the case for the Italian catalogue, as only one background PGA value has been used (at the start of the study period). The paragraph has been rewritten to account for this explanation:

"*In this section, models 1t, 2t and 3t (**Table 9**) are tested using the three PGA background values explained previously (and computed in January 1990, December 1998 and May 2011). As it can be seen in **Figure 11** the annual probabilities decrease before Mula earthquake for Lorca site. However, close to the occurrence of the earthquake, it shows a slight increase even in Vera site, although it is 101.4 km away from the earthquake's epicentre. In Murcia site, the RC continuously decreases until five months before the earthquake, when it shows a sharp increase from -75% to -60% in the change of exceedance probability. This change is also seen in the annual and monthly variations of the RC (**Figure 11 zoom in**). After the Mula earthquake the change in probability exceedance remains higher than 20% (even increasing up until 50% in the case of Lorca and 100% in the case of Murcia) for both Lorca and Murcia sites until Lorca earthquake happens. In Vera site, this parameter oscillates about the baseline. After 2011, the RC steadily increases in Vera, whereas in Lorca and Murcia it stays constant after 2019. On the other hand, Model 2t and Model 3t (**Figure 12**) show a similar behaviour to Model 1t, although Model 3t showcases slightly higher exceedance probability before Lorca 2011 earthquake for both Murcia and Lorca sites. It should be noted that the sudden changes in the RC in January 1999 and one month after the Lorca earthquake, i. e., the -60% to 0% increase in January 1999 (for Lorca and Murcia) and the 100% to 0% decrease in June 2011 (for both Lorca and Murcia), are artefacts due to the change in the background PGA and cannot be considered in the analysis. However, the annual* and *monthly variations of the RC shown in **Figure 13** and **Figure 14** allow to see the changes related to the aforementioned earthquakes occurrences."*

As for the differences in the models we agree that they are similar in the behaviour and just small changes can be appreciated in some periods. The main differences can be observed in the annual variations of the RC. The **Figure 11** has been updated to illustrate the discussion of the results by including a zoom in.

What about the sharp decrease in Lorca and Murcia after the Lorca earthquake?

"*It should be noted that the sudden changes in the RC in January 1999 and one month after the Lorca earthquake, i. e., the -60% to 0% increase in January 1999 (for Lorca and Murcia) and the 100% to 0% decrease in June 2011 (for both Lorca and Murcia), are artefacts due to the change in the background PGA and cannot be considered in the analysis.*"

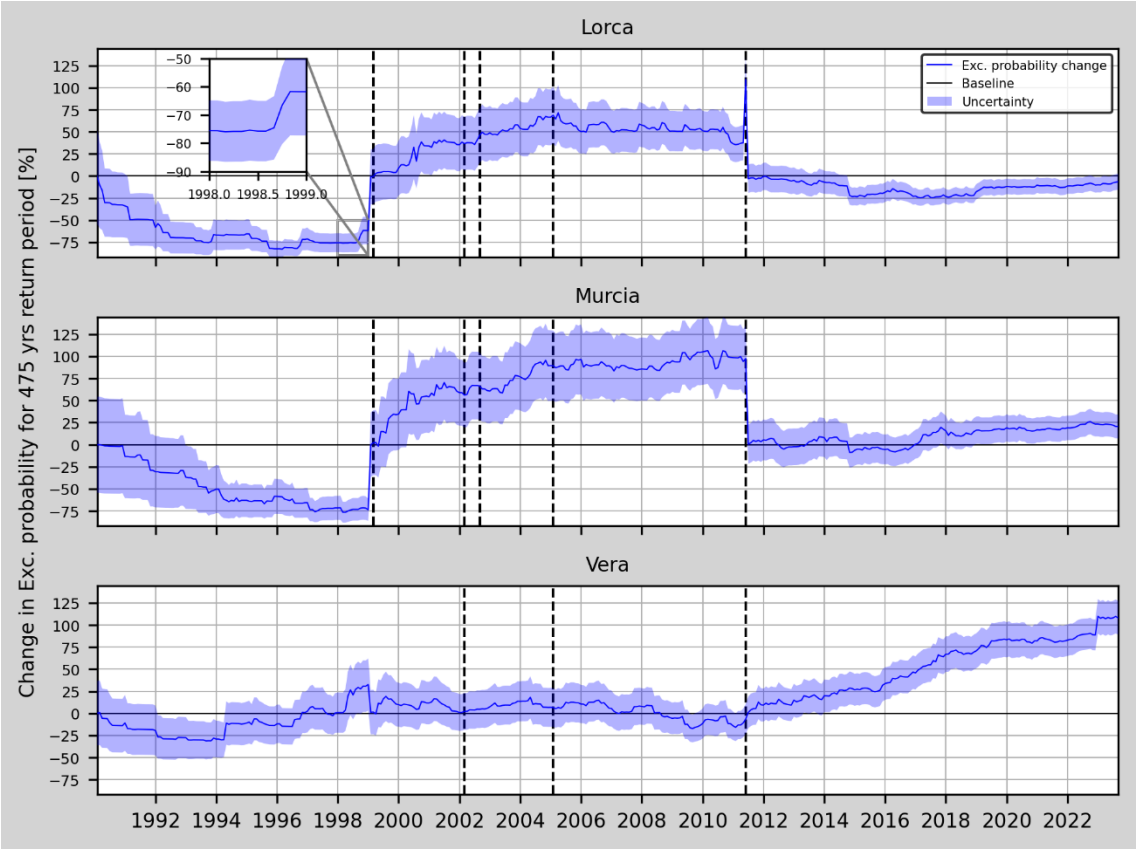

Figure 11. Relative change (RC) of the annual exceedance probability and corresponding uncertainty for Model 1t in Lorca, Murcia and Vera (from top to bottom). The vertical dashed black lines mark the earthquakes considered in Table 5 which are closer than 75 km to each one of the sites. A zoom in on the mentioned increase in the RC during 1998 in Lorca's site appears in the upper left side of the graph.

The symbology in **Figure 12** has been changed so that the Model 3t is better seen.

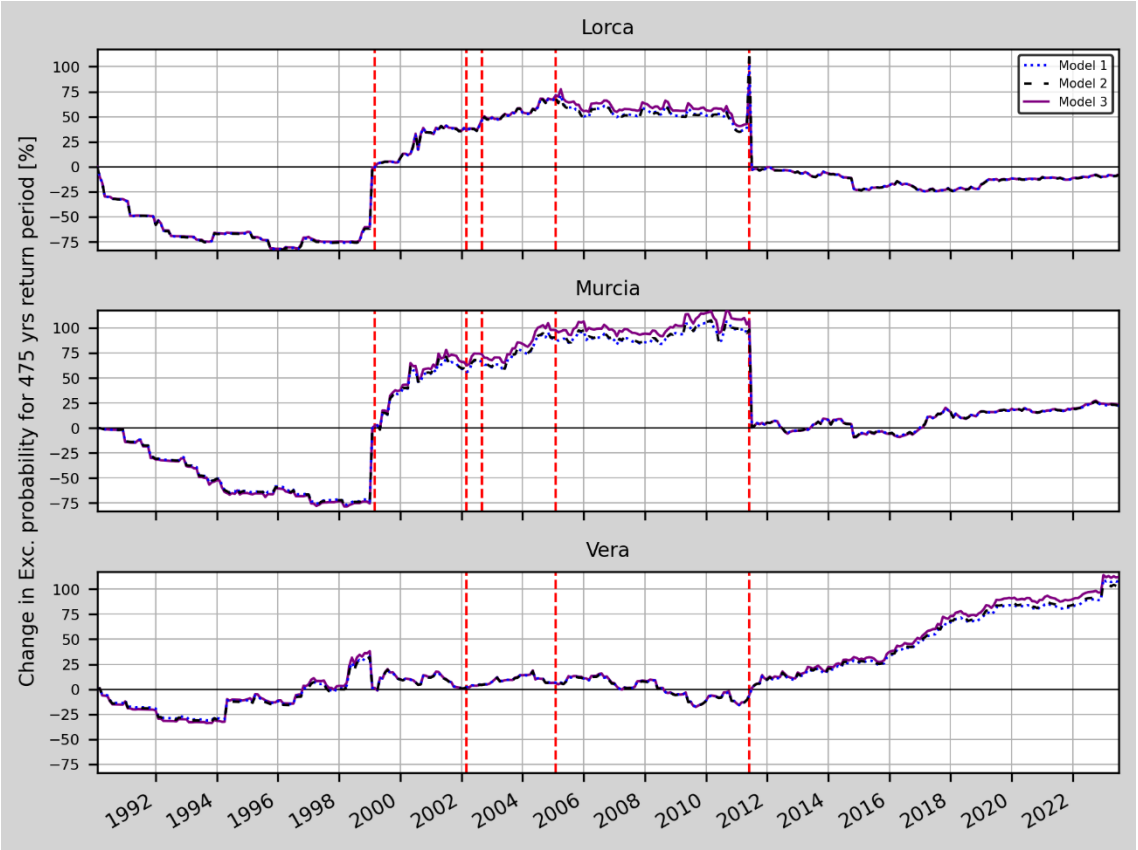

Figure 12. Mean value of the relative change (RC) of the annual exceedance probability for models 1t, 2t and 3t in Lorca, Murcia and Vera (from top to bottom). At the right side, a zoom in on the peak due to Lorca earthquake. The vertical dashed red lines mark the earthquakes considered in Table 5 which are closer than 75 km to each one of the sites.

Page 24: Comment on Figure 13

The paragraph has been rewritten as the **Figure 13** has been modified due to a change in the representation of the data that affected several points in the graph. Lines 378-389:

Is this change significant of just a random variation?

"Figure 13 shows a 20% mean decrease in the annual variation of the RC from January 1991 to March 1993 that could be explained by the RC uncertainty (as can be seen in Figure 11 for both Lorca and Murcia sites, with higher uncertainty for that period). Then, a 15% increase in the annual variation in the RC of the exceedance probability from October 1998 until August 1999 can be seen for Lorca site (three months before Mula earthquake and then six months after it). This increase can also be seen in the declustered catalogue scenarios (Figure 16, Figure A5 and Figure A6). *In Vera site, the increased RC variation during 1999 could be due changes in the b-value from April to December (six earthquakes with magnitude from 3.5 to 3.8 Mw occurred). In the case of Gergal and Bullas earthquakes in 2002 there is no increased variation of the RC. However, it can be seen for Lorca and Murcia sites that from July 1999 to May 2001 that the annual variations of the RC reach values higher than 15% with respect the baseline and with*

a mean value of 10% over this period. This increased values cannot be related with any close seismic activity greater than or equal to 4.0 Mw. It can also be seen that in Lorca site the annual variation stays higher than 20% for one year after Lorca earthquake. Lastly, the peak in the annual and monthly variation at Vera in 2022 appears due to the seismic activity in Turre (a town 14 km south from Vera) where a 4.0 Mw earthquake struck on 31 December 2022."

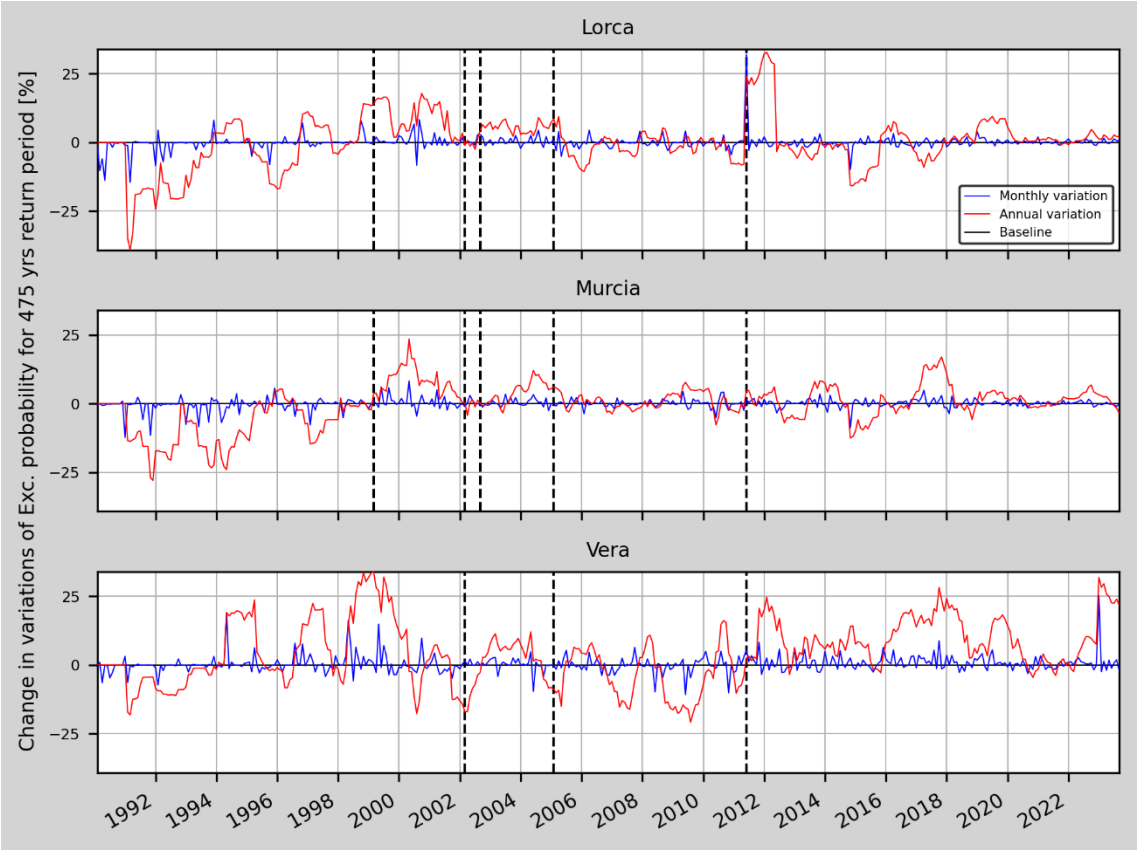

Figure 13. Annual and monthly variations of the relative change of the annual probability of exceedance for Model 1t in Lorca, Murcia and Vera (from top to bottom). The vertical dashed black lines mark the earthquakes considered in Table 5 which are closer than 75 km to each one of the sites.

Pages 25-27: Figures 14 and 15 and comments.

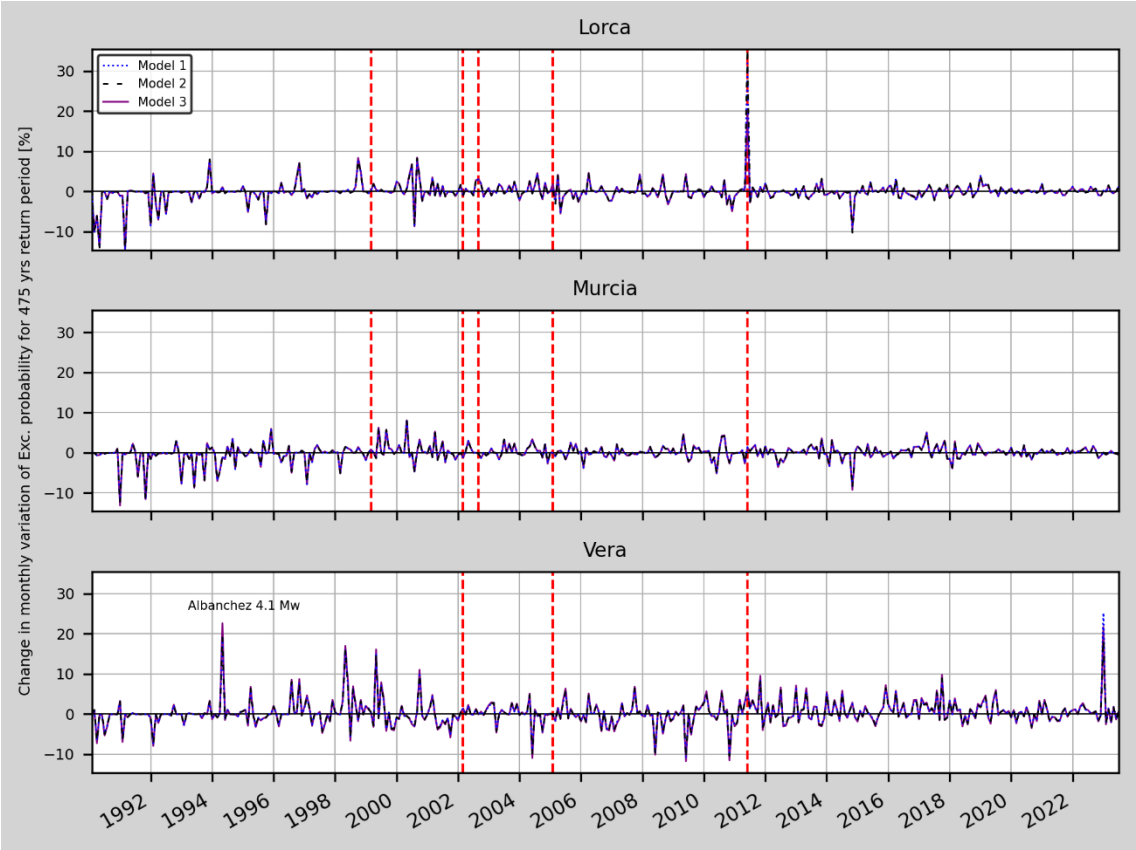

Figure 14. Monthly variations of the relative change of the annual probability of exceedance for models 1t, 2t and 3t in Lorca, Murcia and Vera (from top to bottom). The vertical dashed red lines mark the earthquakes considered in Table 5 which are closer than 75 km to each one of the sites. The earthquake that could cause the peak in 1994 at Vera site has also been indicated.

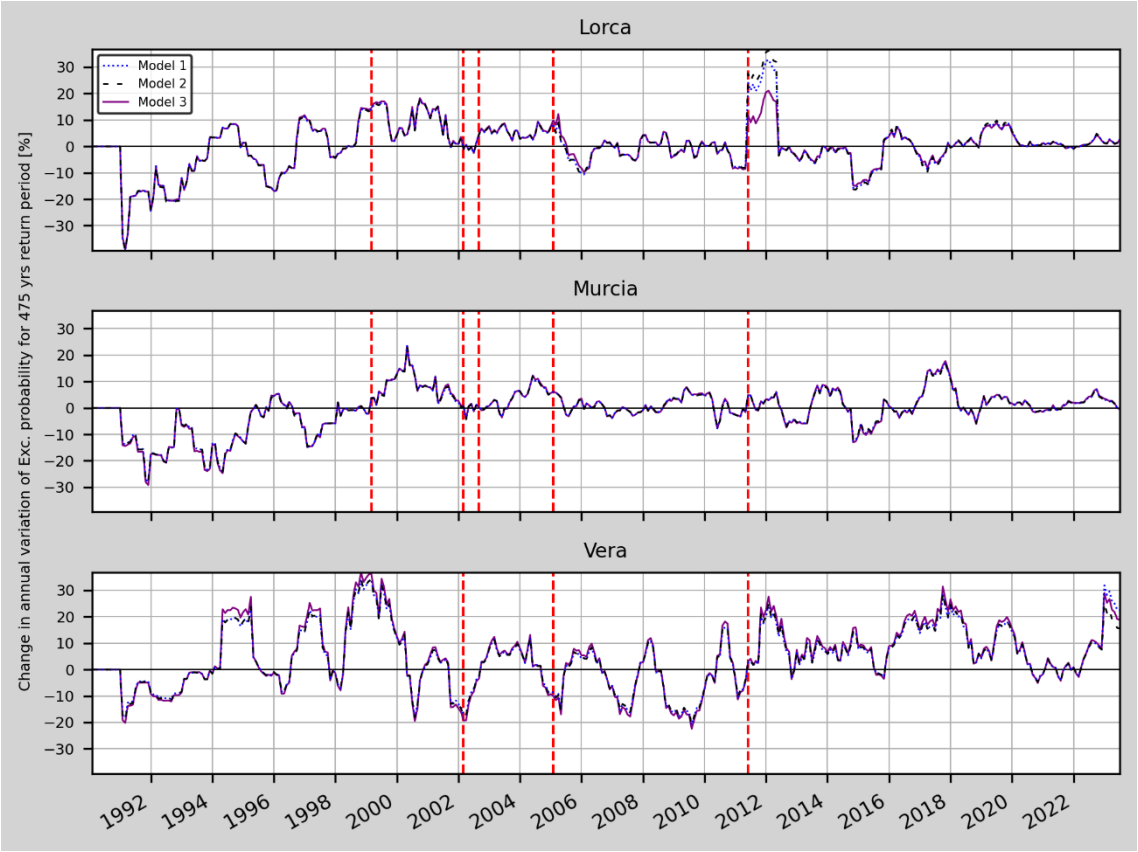

Figure 15. Annual variations of the relative change of the annual probability of exceedance for models 1t, 2t and 3t in Lorca, Murcia and Vera (from top to bottom). The vertical dashed red lines mark the earthquakes considered in Table 5 which are closer than 75 km to each one of the sites.

This figure contains the same plot as in Figure 11 for model 1t.

Page 25

Lines 390-400:

The paragraph has been rewritten as the **figures 14 and 15** have been changed due to a change in the representation of the data that affected several points in the graph:

*"Similar results are obtained for all three locations, although higher changes in the monthly variations (**Figure 14**) can be seen for Model 1t and Model 2t after Lorca's earthquake in Lorca site, and for Model 1t in December 2022 at Vera site. Overall, the monthly variations do not show changes preceding relevant earthquakes. One of the possible explanations is the lack of foreshocks in most of the main shocks. In Lorca earthquake, even though there was a 4.5 Mw earthquake almost two hours before the main-shock, the one-month increments on the computation process are not able to show any change in RC.*

*The annual variations on the other side (**Figure 15**), show periods of increased RC before some of the selected earthquakes. An example is seen in Lorca site where a 15% increase is seen before Mula earthquake from June 1998 (the earthquake occurred in February 1999). Another example can be seen in both Murcia and Lorca*

sites, where a 10% increase can be seen before Aledo earthquake from May 2004 until the earthquake occurrence in January 2005.

The most prominent increase on the annual variation occurs after Lorca earthquake (32.8%, 36.2% and 21% for models 1t, 2t and 3t).”

Page 27: Effect of the declustering on the results.

The second paragraph and the **Figure 16** have been modified in order to help the discussion of the results.

“***Figure 16*** *represents the changes in the annual exceedance probability for Model 1t. As can be seen, the results using a non-declustered catalogue provide lower changes in the exceedance probability for Mw 4.0 in Lorca site from 1996 until 2011. Then, from 2011 until 2023, the non-declustered catalogue provided a higher RC. At both Murcia and Vera, the results are similar for the non-declustered and declustered catalogues. It should also be noted that the mean uncertainty of the RC is slightly higher for the declustered catalogue (a 11.21% for Lorca, -0.41% for Murcia and 5.58% for Vera). Since the results are compatible, keeping the foreshocks and aftershocks, i.e. using the non-declustered catalogue, seems to be a better choice if the aim is to perform OEF. Some of the advantages would be a lower uncertainty in the RC and the possibility of using more detailed time scales in case foreshocks are present.”*

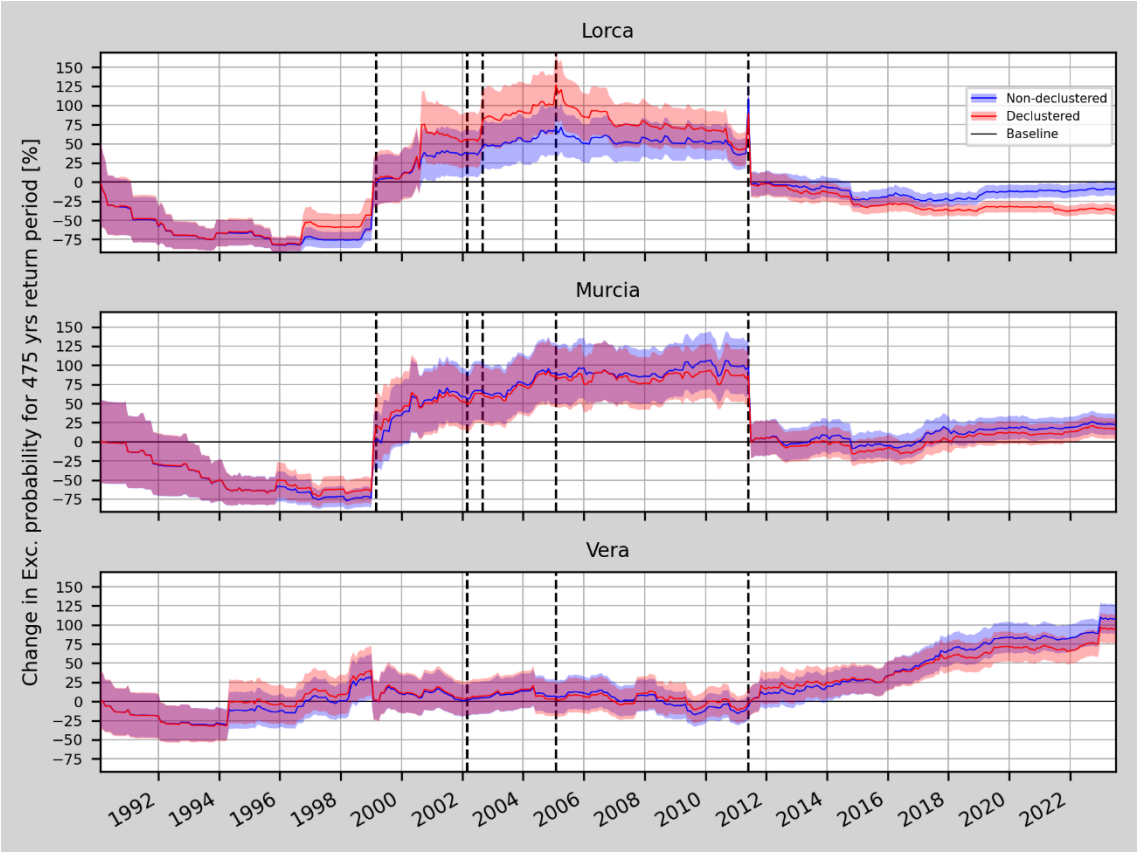

Figure 16. Model 1t. Comparison of the relative change (RC) of the annual exceedance probability and its uncertainty for a non-declustered and a declustered catalogue in Lorca, Murcia and Vera (from top to bottom). The vertical dashed black lines mark the earthquakes considered in Table 5 which are closer than 75 km to each one of the sites.

Page 28-29: Conclusions.

The conclusions have been rewritten:

"*This methodology considers the influence of all the events in the seismic clusters and also the location of the seismic sources (corresponding active faults) for seismic activity rate smoothing and b-value computation, showing that when computing a time-dependent PSHA the use of a non-declustered catalogue will provide similar results to using a declustered catalogue with the added benefit of keeping the foreshock activity. Therefore, if we compute the changes of the annual probability of exceedance for a given PGA value (fixed as a background value which may change according to the updates in the seismic normative), we will be able to show how this probability is changing with time.*

The changes in the annual probability of exceedance (increases and decreases) can be more accurately described using a spatially gridded time-dependent b-value instead of a fixed one for each tectonic zone. This can be seen when comparing ***Figure 10*** *with* ***Figure 12****. Therefore, we suggest using spatially gridded b-values for the corresponding period (time-dependent) when computing the background PGA value and the corresponding changes in the annual probability of exceedance in the time-dependent PSHA.*

Regarding which of the proposed models can be more effectively used to describe these changes, we have to consider several factors. One could be how close are the computed PGA values to the national seismic hazard maps for each country. In the case of Central Italy models 1t, 2t and 3t provide the following background PGA values: 340.61, 359.72 and 334.28 cm/s^2. The ESHM20 model (Danciu et al., 2021) computes 334.38 cm/s^2. The closest match would be Model 3t followed by Model 1t. However, by looking at ***Figure 5*** *and* ***Figure 7****, it can be seen that the Model 3t seems to be less affected by changes in the seismic activity than Model 1t, as the monthly and annual RC variations suggest (Model 1t monthly and annual variations are 4.5 times higher than Model 3t variations'). With this information Model 1t seems appropriate for the purpose of this work.*

In general, this methodology benefits from complete catalogues in zones with increased seismicity - assuring less uncertainty in the b-value computation - and well-defined seismicity sources, where the seismicity smoothing is accurate. ***Figure 16*** *shows this result, as the non-declustered catalogue (with weighted down cluster events) has less RC uncertainty and enables the use of the foreshocks in daily to weekly time scales."*

Probably due to the foreshock period before the mainshock.

Although our results are not significant to relate these changes to the occurrence of a main earthquake for low to moderate seismicity areas, the methodology can be useful for other countries with a higher seismicity, or in the future if new significant earthquakes occur in the studied region of Spain. ***As we saw, for Central Italy both the annual and monthly changes of the exceedance probability show important variations related to the foreshock activity preceding L'Aquila earthquake. This could be useful for OEF****.*

Finally, in the case of south-eastern Spain, the PSHA kept high in the region after the Mula earthquake and did not decrease until the occurrence of the Lorca earthquake. However, the continuous increase of the PSHA in Vera after the Lorca earthquake cannot be directly related to a potential upcoming earthquake similar to the one from Lorca. Therefore, more time and data are needed to confirm this."

A better interpretation of the results is needed. Why sometimes the PSHA increase after a mainshock and other times it decreases suddenly?

Response in pages 8 and 9 of this document.

Page 34-35: Appendix A2 Effect of the declustering on the results

Figure A5 has been corrected as Lorca's site data was erroneous.

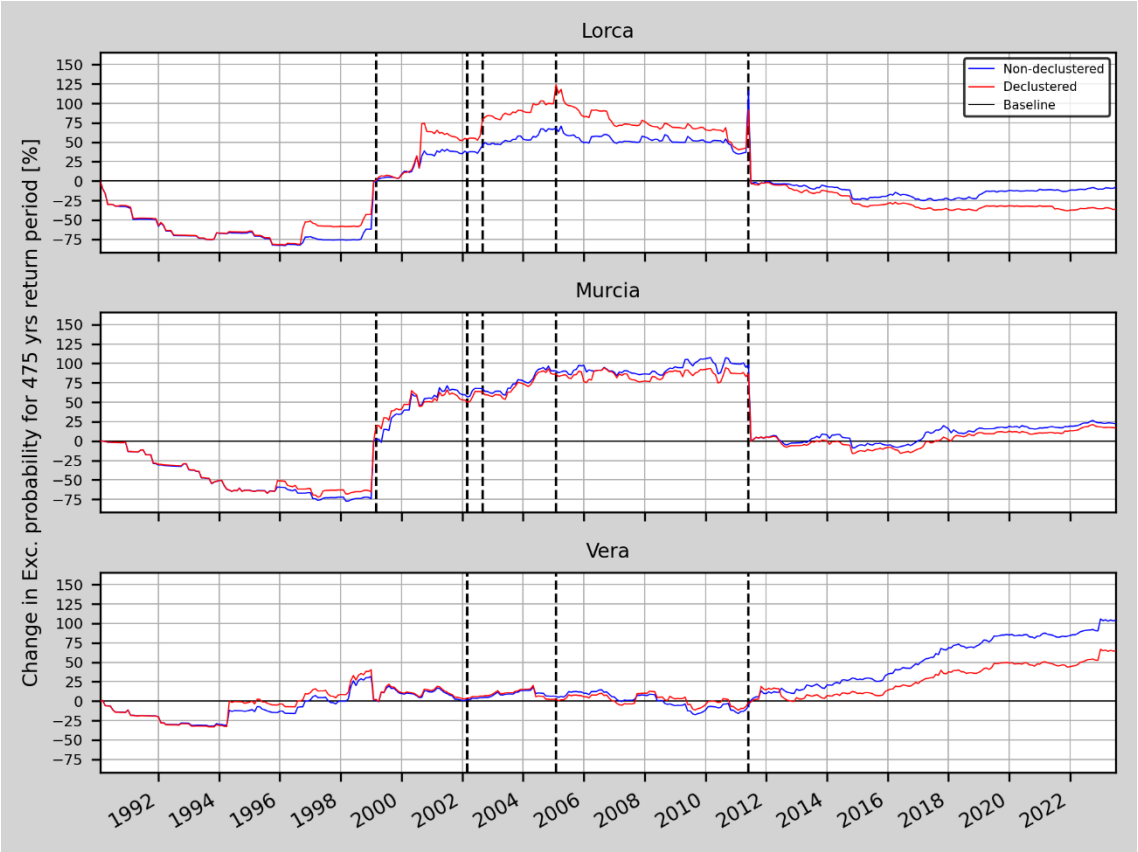

Figure A5. Model 2t. Relative change (RC) of the annual exceedance probability for a non-declustered and a declustered catalogue in Lorca, Murcia and Vera (from top to bottom).

References added:

Hiemer, S., Woessner, J., Basili, R., Danciu, L., Giardini, D., and Wiemer, S.: A smoothed stochastic earthquake rate model considering seismicity and fault moment release for Europe, Geophysical Journal International, 198, 1159-1172, https://doi.org/10.1093/gji/ggu186, 2014

Zhuang, J., Ogata, Y., and Vere-Jones, D.: Stochastic declustering of space-time earthquake occurrences, J. Am. Stat. Ass. 97, 458, 369–380, 2002

Marsan, D. and Lengliné, O.: Extending earthquakes' reach through cascading, Science 319, 1076–1079, 2008.

Console, R., Jackson, D. D. and Kagan, Y. Y.: Using the ETAS model for catalog declustering and seismic background assessment. Pure Appl. Geoph., 10.1007/s00024-010-0065-5., 2010.

Second Reviewer

First of all, thank you, Prof. Chan, for your comments and suggestions in the review of the manuscript. In the following document, all the questions will be answered in order and quoting each item of the review using the yellow highlighted and bold font style. The numeration has changed and the figures' and tables' numeration refers to the last version of the manuscript.

The Italy case not discussed: The abstract and various sections of the manuscript mention the application of this approach to the L'Aquila, Italy, case. However, I am unable to find any corresponding results or discussion.

The corresponding paragraphs (section **3.1.2 Results** and **4.0 Conclusions**) have been modified in order to discuss the results from Central Italy case.

3.1.2 Results

*"**Figure 5** (Model 1t) presents a moderate increase in the annual exceedance probability (25%) one month before L'Aquila earthquake occurred, and not only the annual but also the monthly variation of relative change reaches values higher than 35%. This sudden change is most probably due to the foreshock activity that preceded the mainshock, as a 4.1 M_L ground motion occurred on 30 March 2009. **Figure 6** (Model 2t) shows a similar trend in all the metrics as the previous model with a slightly lower value for the exceedance probability change before the earthquake (22%) and the annual and monthly variations (32%). The Model 3t (**Figure 7**) provides the lowest values for the metrics (-3%, 4% and 3%, respectively). After this increase the RC slowly decreases over time for all three models."*

4.0 Conclusions

[…]

*"Regarding which of the proposed models can be more effectively used to describe these changes, we have to consider several factors. One could be how close are the computed PGA values to the national seismic hazard maps for each country. In the case of Central Italy models 1t, 2t and 3t provide the following background PGA values: 340.61, 359.72 and 334.28 cm/s^2. The ESHM20 model (Danciu et al., 2021) computes 334.38 cm/s^2. The closest match would be Model 3t followed by Model 1t. However, by looking at **Figure 5** and **Figure 7**, it can be seen that the Model 3t seems to be less responsive to the seismic activity than Model 1t, as the monthly and annual RC variations suggest (Model 1t monthly and annual variations are 4.5 times higher than Model 3t variations'). With this information Model 1t seems appropriate for the purpose of this work.*

*In general, this methodology benefits from complete catalogues in zones with increased seismicity - assuring less uncertainty in the b-value computation - and well-defined seismicity sources, where the seismicity smoothing is accurate. **Figure 16** shows this result, as the non-declustered catalogue (with weighted down cluster events) has less RC uncertainty and enables the use of the foreshocks in daily to weekly time scales.*

Although our results are not significant to relate these changes to the occurrence of a main earthquake for low to moderate seismicity areas, the methodology can be useful for other countries with a higher seismicity, or in the future if new significant earthquakes occur in the studied region of Spain. As we saw, for Central Italy both the annual and monthly changes of the exceedance probability show important variations related to the foreshock activity preceding L'Aquila earthquake. This could be useful for OEF."

[…]

Definition of smoothing kernel: In this study, the smoothing kernel is determined by the average distance between all events surrounding an earthquake and the precision of the epicenter's location (Lines 68-70). When defining the second moment of the distribution (Sec. 2.1.2), this parameter is solely attributed to the precision of the earthquake epicenter measurement. However, I anticipate that the distance between all events is equally important for this parameter.

The smoothing kernel section and subsections have been rewritten in order to explain some of the features as well as to address this matter. Find here, the part of interest as well as the figure comparing the different cases (that arise from the different geometries and relations between faults). The rest of the modifications can be found in the modified version of the manuscript attached to the response.

- **Second moment of the distribution, σ** has been renamed to **Geophysical meaning of the parameter σ** and the contents of the subsection have been rewritten in order for them to be more clearly defined.

"This parameter accounts for the dispersion of the values of the distribution around the mean value. That is to say, how far one might expect to find earthquakes around the most probable value (of distance). Therefore, we have considered that this second parameter is related to the accuracy of earthquake's epicentre measurement. This means that it would depend on the methodologies and instrumentation used for the calculation of the epicentre, and thus, on both the year and the location of the catalogue.

It should be noted that σ may depend on other geophysical parameters such as the characteristics of ground, the style of faulting and/or the tectonic stress regime, to cite a few. Nevertheless, in this work only the influence of the uncertainty in the epicentre's location will be considered in the smoothing process.

*As in the previous section, two different options regarding the epicentre uncertainty, **ε**, have been considered: either it depends on the year of occurrence (**ε_1**), or it is constant and computed as the mean value of the epicentral uncertainty for all the events (**ε_2**). "*

A new subsection has been added to show examples of the smoothing kernel implementation and a figure showcasing how the smoothing works is presented:

2.1.3 Examples of implementation

"In this section, some examples of how the smoothing kernels works are shown. There are three main different manners in which this smoothing is applied:

- *Usual 1D Gaussian filter,* $\mu = 0$

This is the case when using models 2 and 3 also when the distance from the centre of the spatial grid cell in which the seismic activity rate is computed to the nearest fault is greater than $\boldsymbol{d_c}$ *as defined in the section* ***2.1.1.*** *An example can be seen in* ***Figure 1a.***

- *Single fault,* $\mu \neq 0$

When the nearest fault is closer than $\boldsymbol{d_c}$ *from the centre of the spatial grid cell then the resulting function will provide a ring-shaped smoothed activity, the width of which will depend on* $\boldsymbol{\sigma}$*. Only the section of this ring in which the fault is located will be used in the smoothing. This can be achieved by considering the* $\boldsymbol{n}$ *closest points to the spatial grid cell centre and then computing the angles to define the ring arc (****Figure 1b****).*

- *Several faults,* $\mu \neq 0$

*This case is a generalization of the former with the exception that when spatial grid cell's centre is in between faults and at similar distances, then the full ring will be used as smoothing function (****Figure 1d****). On the other hand, if the distance to both faults is similar, but the spatial grid cell's centre is not in between the faults then the resulting smoothing is a ring arc (****Figure 1c****)."*

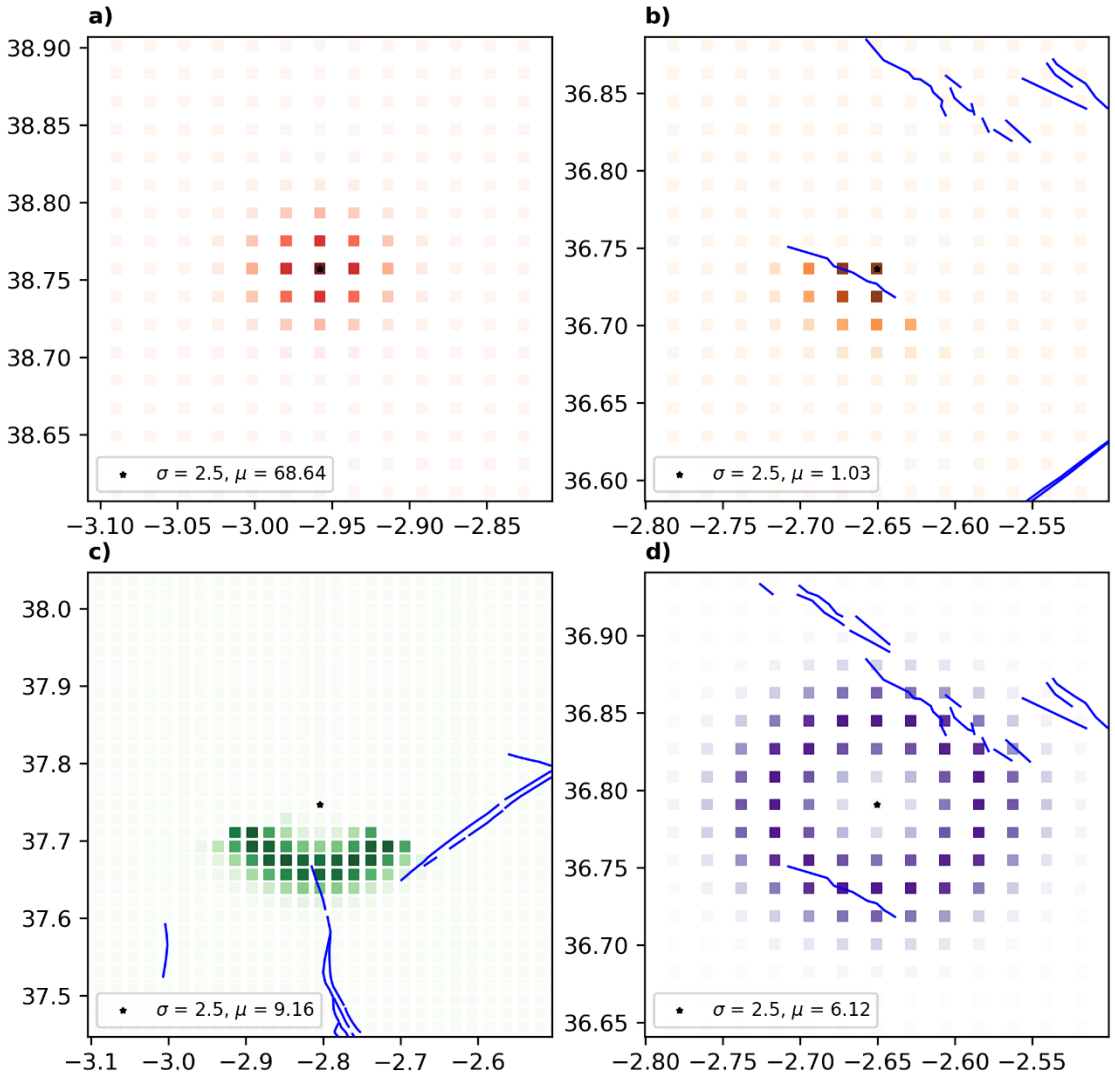

Figure 1. a) Smoothing function for $\mu = 0$. b) Smoothing function for $\mu \neq 0$ and a single fault. c) Smoothing function for $\mu \neq 0$ and several faults at similar distances. d) Smoothing function for $\mu \neq 0$ and the spatial grid cell in between faults at similar distances. The blue lines show the fault traces. In this example d_c equals 48 km.

Completeness magnitude: Based on my interpretation of Table 7, it appears that the magnitude range indicated in the top column has been complete from the year specified in the bottom column. Therefore, it should be that magnitudes of 3.0 and above are complete since 1978, rather than starting from magnitude 3.25 as stated in Lines 277-280. Additionally, the completeness magnitude typically decreases with upgrades to the seismic network, as such improvements generally enhance detection capabilities. It is customary for the completeness magnitude to remain stable for approximately a decade before decreasing sharply with a network upgrade. The gradual increase in the average completeness magnitude observed in Table 8 is unexpected. An explanation for the trend of decreasing completeness magnitude would be beneficial.

We agree that this should be the case. The data used for the tables has two different sources with an overlapping period (1962-1979). The difference in the values is due to the extent of each period. For instance, in **Table 7** the values 3.25 and 3.75 Mw

are the class marks for the years 1978 and 1975, respectively. Meanwhile, in **Table 8** the corresponding completeness magnitude value for the period from 1962 to 1979 is 3.4 Mw and has been computed as the spatial average for the South-eastern Spain area using the data from ***(González, 2017).*** This procedure combined with an inequal development of the seismic network could explain the smooth changes in the completeness magnitude.

The completeness magnitude values used in this work are the following and now appear as a single table in the manuscript, note that the values from ***Gaspar-Escribano et al. (2015)*** corresponding to the years 1975 and 1978 have not been used as the data from ***(González, 2017)*** allows to further discretize the timeline:

Years	1048-1520	1521-1800	1801-1883	1884-1908	1909-1962	1963-1979	1979-1984
Completeness magnitude [M_w]	6.25	5.75	5.25	4.75	4.25	3.4	3.3

Years	1984-1992	1993-1998	1998-2002	2002-2010	2010-2013	2013-2023
Completeness magnitude [M_w]	3.0	2.9	2.3	2.1	1.9	1.8

The abrupt change between the period 1909-1962 and 1963-1979 is to be expected, as more development in the seismic network had been made in the mid-20th century than in the early 20th century given the political and historical context of Spain.

The paragraph before the table has been modified to explain the values used in this work.

*"**Gaspar-Escribano et al. (2015)** defined different threshold magnitudes for different regions around Spain. The class marks of these magnitude intervals for the zone of interest (South-eastern Spain) have been selected as the completeness magnitudes up until 1962. From 1962 on, the completeness magnitude has been computed by spatially averaging the gridded completeness magnitude results available from **González (2017)** over the area of study. The completeness magnitude values used in this work are presented in **Table 7**."*

*Table 7. Completeness magnitude for each period according to **Gaspar-Escribano et al. (2015)** in the top tabular and the spatially averaged completeness magnitude for each period using the results from **González (2017)** in the bottom tabular.*

Completeness magnitude [M_w]	6.25	5.75	5.25	4.75	4.25
From year	1048	1521	1801	1884	1909
to year	1520	1800	1883	1908	1962

Completeness magnitude [M_w]	3.4	3.3	3.0	2.9	2.3	2.1	1.9	1.8
From year	1963	1980	1985	1993	1999	2003	2011	2013
To year	1979	1984	1992	1998	2002	2010	2013	2023

Model validation: Based on the results presented for the three models concerning both annual and monthly variations in the change of exceedance probability (as seen in Figures 12 and 13 and discussed in Lines 335-337), the authors assert that Model 1t outperforms the others. However, discerning significant differences is challenging, whether in the monthly variations of the relative change in annual probability of exceedance (Figure 12) or in the annual variations of the same (Figure 13). Moreover, I question the approach of basing model validation solely on 'greater changes before and after selected earthquakes' without incorporating statistical analyses. I believe that a more rigorous statistical evaluation is necessary to substantiate the claimed superiority of Model 1t.

We agree that the discussion of the models' performance should be further explained. To do so, the figures of the results have been modified in order to be clearer and the results have commented in their respective sections and also in the conclusions.

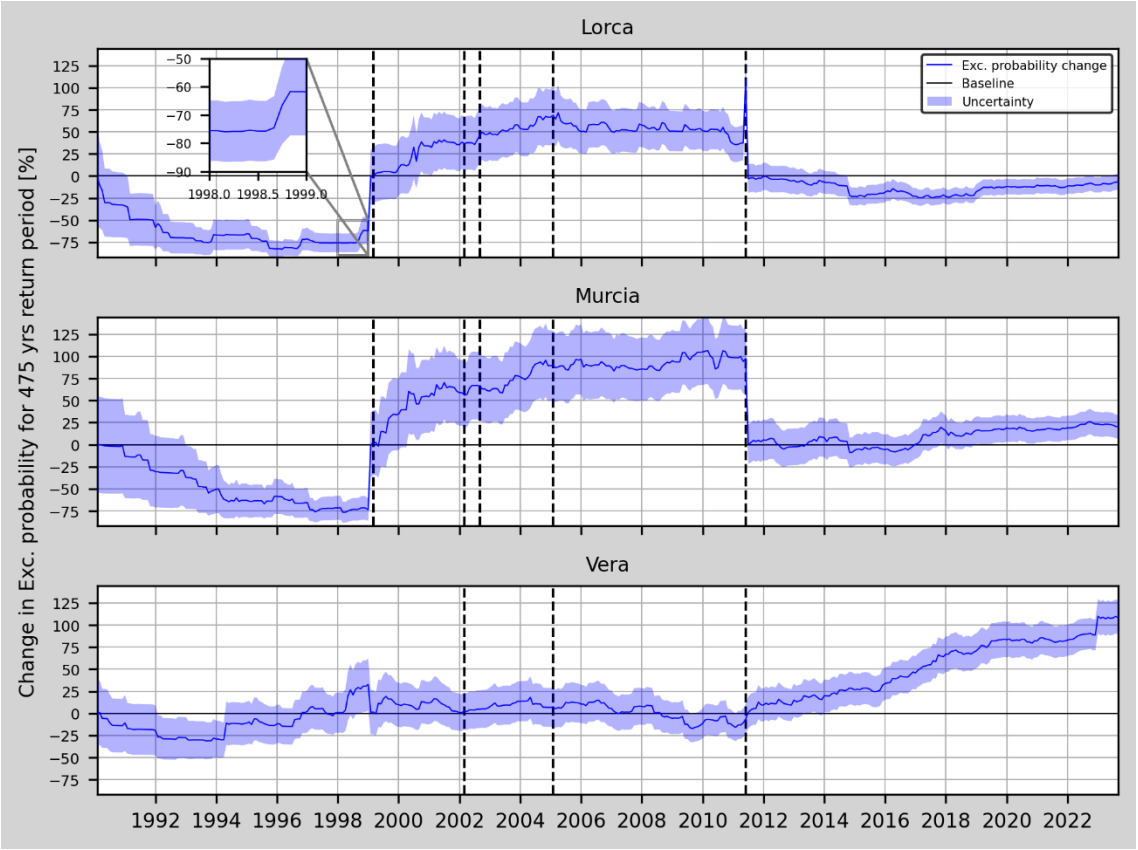

Figure 11. Relative change (RC) of the annual exceedance probability and corresponding uncertainty for Model 1t in Lorca, Murcia and Vera (from top to bottom). A zoom in on the mentioned increase in the RC during 1998 in Lorca's site appears in the upper left side of the graph.

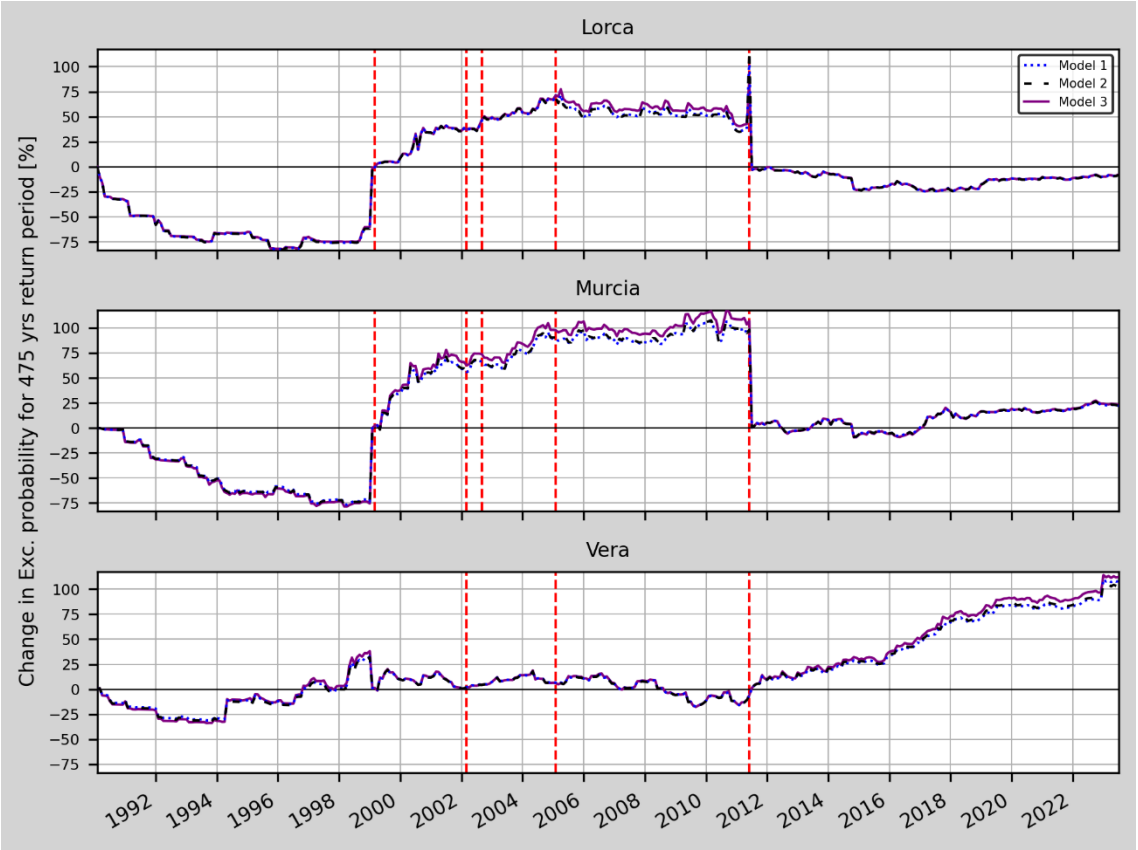

Figure 12. Mean value of the relative change (RC) of the annual exceedance probability for models 1t, 2t and 3t in Lorca, Murcia and Vera (from top to bottom). At the right side, a zoom in on the peak due to Lorca earthquake.

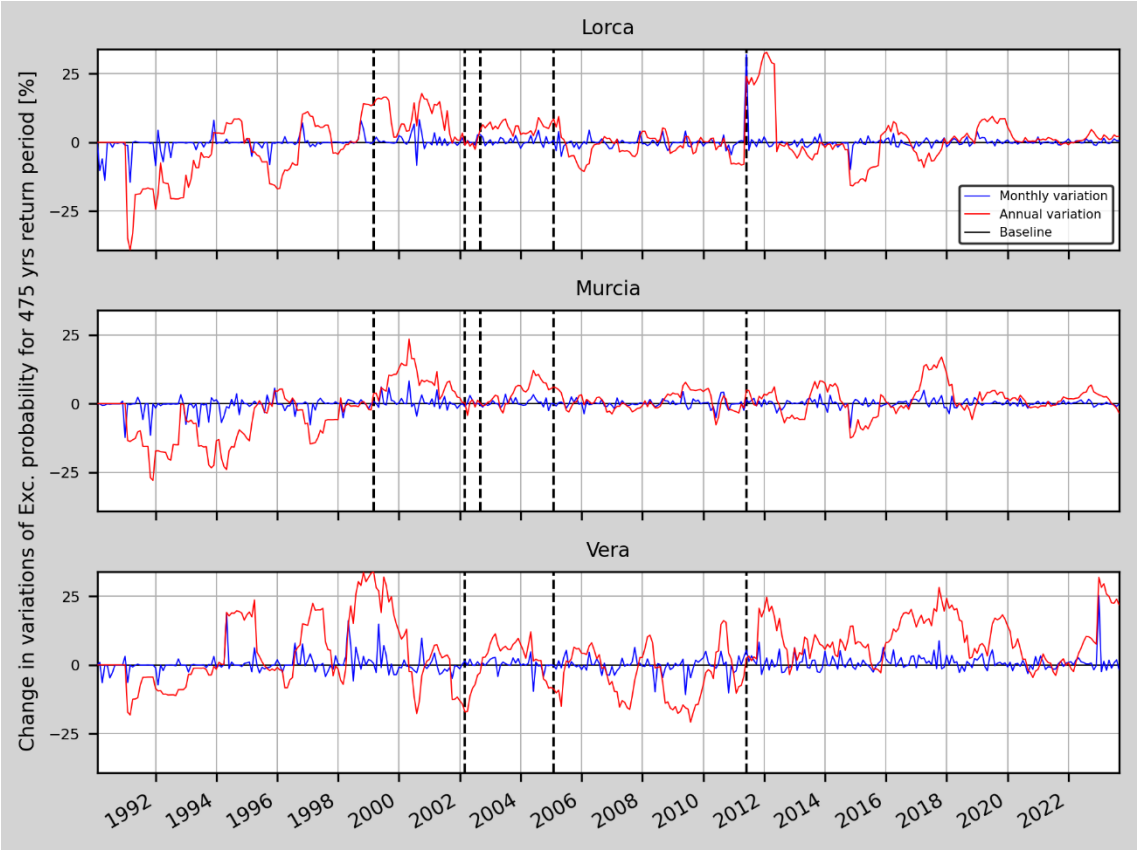

Figure 13. Annual and monthly variations of the relative change of the annual probability of exceedance for Model 1t in Lorca, Murcia and Vera (from top to bottom).

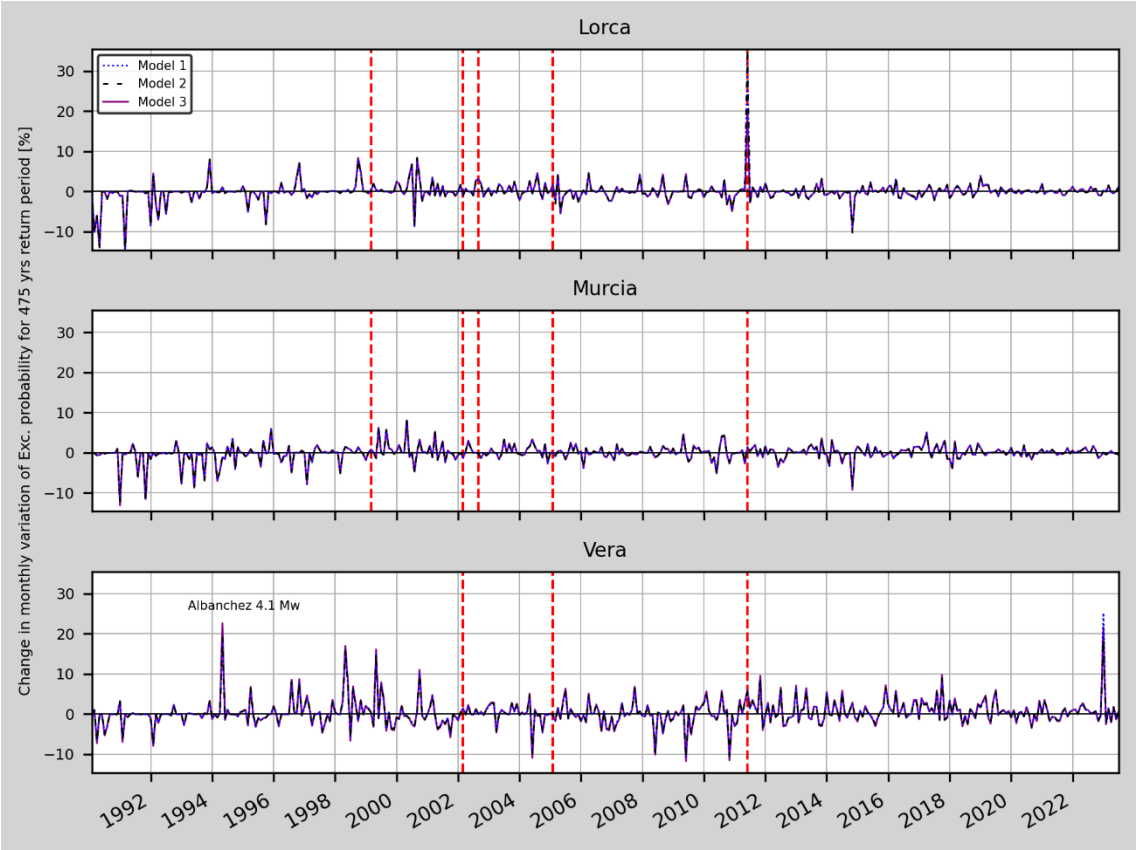

Figure 14. Monthly variations of the relative change of the annual probability of exceedance for models 1t, 2t and 3t in Lorca, Murcia and Vera (from top to bottom). Two peaks have been selected for a zoom in detail (after Lorca earthquake in Lorca site and in December 2022 in Vera site). The earthquake that causes the peak in 1994 at Vera site has also been indicated.

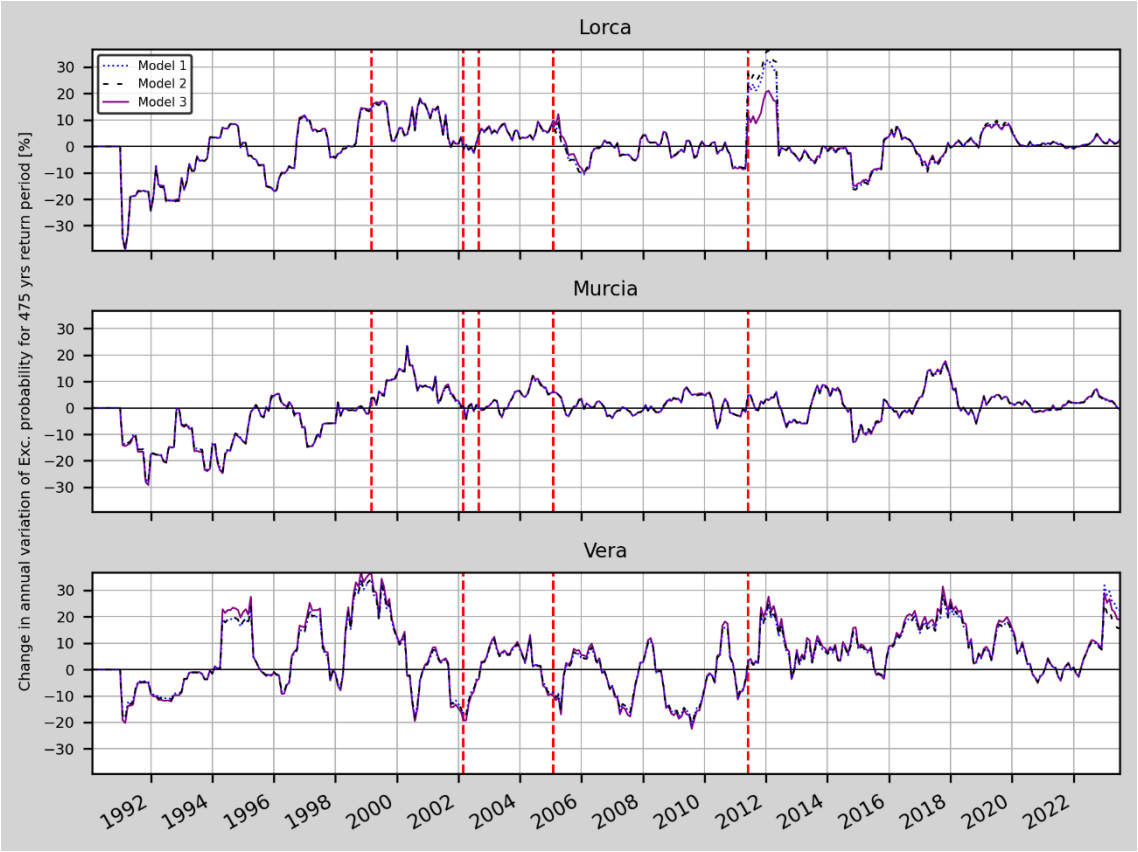

Figure 15. Annual variations of the relative change of the annual probability of exceedance for models 1t, 2t and 3t in Lorca, Murcia and Vera (from top to bottom).

*"Similar results are obtained for all three locations, although higher changes in the monthly variations (**Figure 14**) can be seen for Model 1t and Model 2t after Lorca's earthquake in Lorca site, and for Model 1t in December 2022 at Vera site. Overall, the monthly variations do not show changes preceding relevant earthquakes. One of the possible explanations is the lack of foreshocks in most of the main shocks. In Lorca earthquake, even though there was a 4.5 Mw earthquake almost two hours before the main-shock, the one-month increments on the computation process are not able to show any change in RC.*

*The annual variations on the other side (**Figure 15**), show periods of increased RC before some of the selected earthquakes. An example is seen in Lorca site where a 15% increase is seen before Mula earthquake from June 1998 (the earthquake occurred in February 1999). Another example can be seen in both Murcia and Lorca sites, where a 10% increase can be seen before Aledo earthquake from May 2004 until the earthquake occurrence in January 2005.*

The most prominent increase on the annual variation occurs after Lorca earthquake (32.8%, 36.2% and 21% for models 1t, 2t and 3t)."

In the conclusions, also:

4.0 Conclusions

[…]

"Regarding which of the proposed models can be more effectively used to describe these changes, we have to consider several factors. One could be how close are the computed PGA values to the national seismic hazard maps for each country. In the case of Central Italy models 1t, 2t and 3t provide the following background PGA values: 340.61, 359.72 and 334.28 cm/s^2. The ESHM20 model (Danciu et al., 2021) computes 334.38 cm/s^2. The closest match would be Model 3t followed by Model 1t. However, by looking at ***Figure 5*** *and* ***Figure 7****, it can be seen that the Model 3t seems to be less responsive to the seismic activity than Model 1t, as the monthly and annual RC variations suggest (Model 1t monthly and annual variations are 4.5 times higher than Model 3t variations'). With this information Model 1t seems appropriate for the purpose of this work."*

Figure 1 caption: Please provide clear definitions for each symbol and color used.

The figure's caption has been updated to include clear definitions for each element of the map. Some changes in the figure have also been made, as some items where not able to be correctly read.

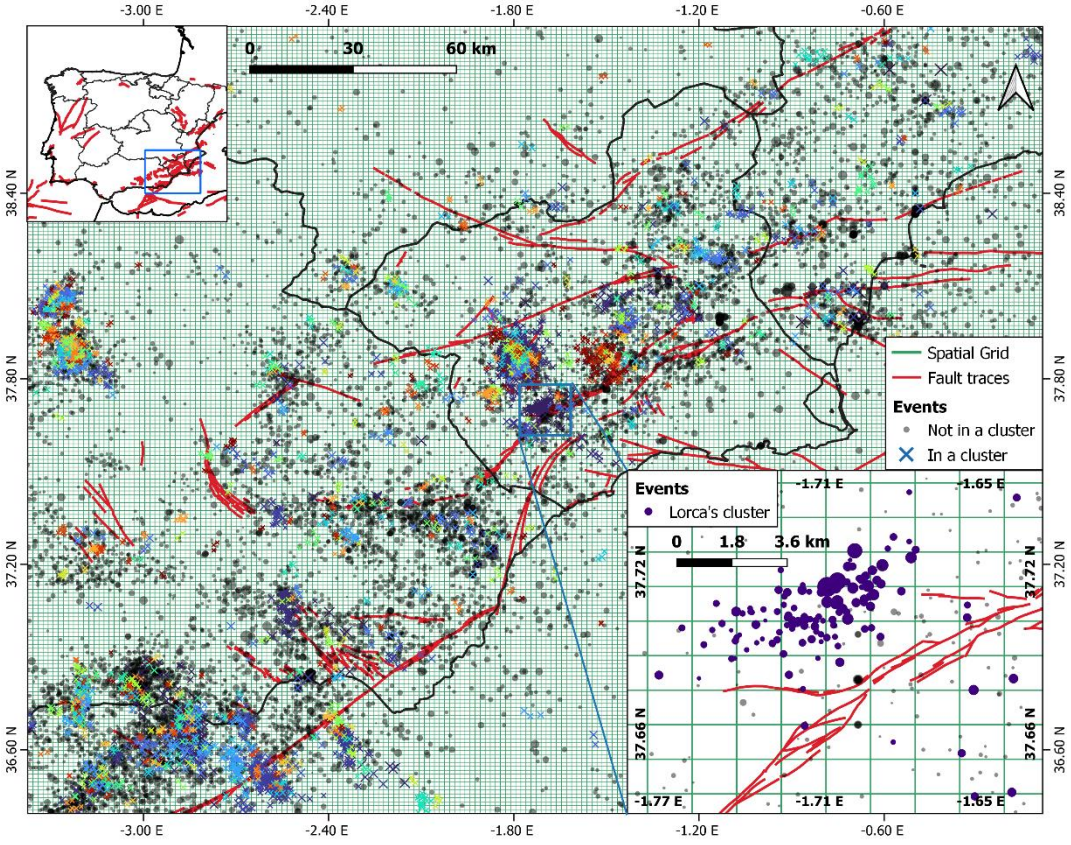

Figure 2. Example of cluster identification in South-eastern Spain. ***The cross markers represent the earthquakes and are coloured depending on the cluster they belong to. The events of the catalogue that do not belong to any cluster are***

represented with grey circles. The fault traces are presented in red-coloured lines and the spatial grid cell's limits with green lines. A zoom in on Lorca's cluster is shown in the bottom right corner, where the events of the Lorca's series are plotted using purple circle symbols.

Lines 159: I am not quite sure if equation (7) is essential.

We agree that it is indeed not essential, the equation 7 has been discarded, although the explanatory paragraph has been kept in order to support **Equation 8** (now **Equation 7**) explanation.

*"To do this, all the events belonging to each cluster are counted and define the clustering weight, c_j. If an event does not belong to any cluster (i.e., the cluster label for that event is set to zero) then c_j equals 1. The weighted counts for each spatial grid cell are calculated as the summation of all the events over the different clusters (**Eq. 7**):"*

Line 182: Revise 'time-dependent' as 'stability'.

In order to be clearer about the b-value options the previous line has been rewritten as:

*"[...] a fixed and **constant** (time-independent) b-value assigned from the tectonic zones of each country [...]"*

We think it is better to keep the time-dependent adjective to the time-dependent model to emphasize the aim of the work, TDPSHA.

Figure 3 caption: Is the tectonic b-value obtained by EHSM20 or by this study?

Yes, the b-values are defined within the tectonic zonation from Danciu et al. (2021) -the EHSM20. In order to clarify this, the caption has been modified.

"The map shows the tectonic zones (green lines) in Central Italy with their acronyms and tectonic b-values as computed in the EHSM20 (Danciu et al., 2021). The star marks the epicentre of L'Aquila earthquake (Table 2), and the red lines represent the fault traces."

Figure 4 caption: Please provide clear definitions for the dashed line.

Figures from Figure 4 until the ones from the appendix have gotten their captions updated in order to have all the information needed for their analysis.

Table 6: The effectiveness of the declustering approaches can be assessed with a confusion matrix, which provides not only the number of events but also the counts of true positives, true negatives, false positives, and false negatives.

A figure presenting the confusion matrix for each of the declustering methods and the discussion, is now presented:

*"Considering that **Cabañas et al. (2011)** carried out a detailed study on the 2011 Lorca's earthquake seismic series, we have used their results to validate the best algorithm. According to them, the cluster corresponding to Lorca's series, from 11 May 2011 until 19 July 2011, is composed of 146 events (including the foreshock, the main shock and the aftershocks). In order to test the performance of the methods, the confusion matrices for each one have been computed. In the area of study, a total of 249 events have been recorded, which means a total of 103 background events should be identified. For this analysis, all the events classified in a cluster different from the one of Lorca series have been considered as background for simplicity. **Figure 9** shows that GK74 method is the most adequate (with a 94.43% mean for the metrics compared with the 92.88% for RJ and a 74.54% for A) and also the one that is able to identify more events belonging to Lorca's series."*

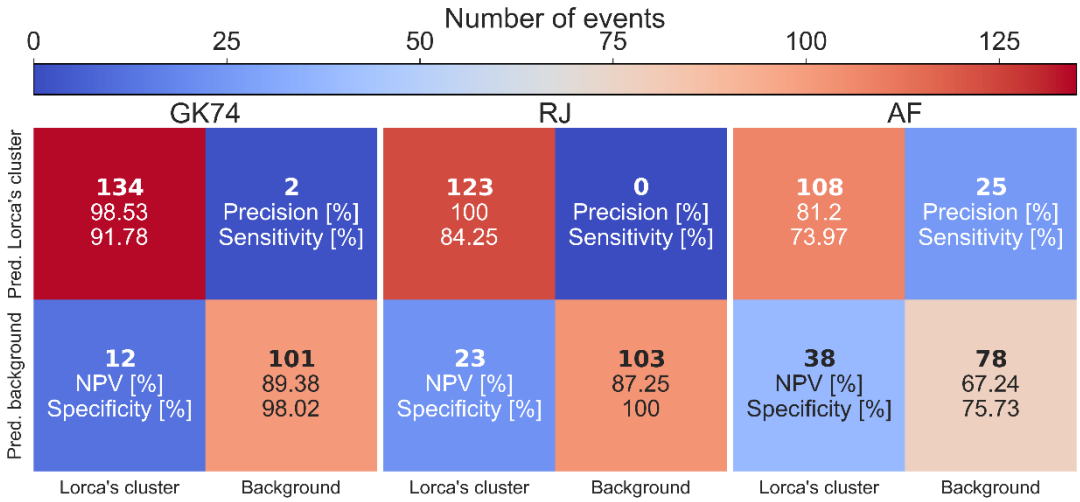

Figure 9. Confusion matrices for the tested declustering methods. Inside each square, the number of events (bold) and some metrics computed using the data are presented (NPV stands for Negative Predictive Value).

Figures 14 and A1, Lines 370-372: Why is there an increase in the expected hazard and rate in Vera? Does this suggest that a large earthquake is anticipated in the future? An explanation based on the data and/or methodology used would be helpful.

The sudden increase in December 2022, that adds up to the increasing RC tendency from 2012 onwards, can be related to the recent earthquake in a municipality 14 km from Vera site. This has been now addressed in the results' comments:

"[...] Lastly, the peak in the annual and monthly variation at Vera in 2022 appears due to the seismic activity in Turre (a town 14 km south from Vera) where a 4.02 Mw earthquake struck on 31 December 2022."

As for the increasing tendency itself, there is not enough data in order to formulate a hypothesis. It could be due to changes in the background seismicity (meaning a new update is due for the PGA background in Vera). In the last paragraph of the conclusions:

"Finally, in the case of south-eastern Spain, the PSHA kept high in the region after the Mula earthquake and did not decrease until the occurrence of the Lorca earthquake. However, the continuous increase of the PSHA in Vera after the Lorca earthquake cannot be directly related to a potential upcoming earthquake similar to the one from Lorca. Therefore, more time and data are needed to confirm this."